

# Formation of N<sub>2</sub>O in Circulating Fluidized Bed Boilers

L.-E. Åmand,\* B. Leckner, and S. Andersson

Department of Energy Conversion, Chalmers University of Technology, S-412 96 Göteborg, Sweden

Received May 8, 1991. Revised Manuscript Received July 29, 1991

The N<sub>2</sub>O formation in circulating fluidized bed boilers is assumed to be influenced by two formation routes, either by char or by hydrogen cyanide originating from the fuel volatiles. A test program was carried out with the purpose of better understanding the formation routes. The test program consisted of step response tests in a 12-MW circulating fluidized bed boiler. Concentration profiles of O<sub>2</sub>, CO<sub>2</sub>, CO, NO, HCN, NH<sub>3</sub>, and C<sub>1</sub> to C<sub>3</sub> hydrocarbons in the combustion chamber of the boiler were also measured in order to support the conclusions of the step response tests. The importance of the two routes is discussed, but no definite conclusions can be drawn about their magnitude.

## Introduction

One of the advantages of fluidized bed combustion (FBC) is the low emissions of NO and SO<sub>2</sub>, a consequence of the combustion temperatures of 800–900 °C which are low in comparison with the temperatures of flame combustion, 1000–1600 °C. The low temperatures in FBC prevent thermal NO formation and promote NO-reducing reactions during the combustion process. The temperature range is also suitable for sulfur capture by limestone addition.

The circulating type of FB boiler (CFB boiler) takes even better advantage of these properties<sup>1</sup> and interest has gradually been focused on this type of boiler. However, the advantage of the lower emissions of NO and SO<sub>2</sub> has lately been found to be offset by high emissions of N<sub>2</sub>O from FB boilers,<sup>2</sup> although not from other combustion equipment.<sup>3</sup> N<sub>2</sub>O is one of the greenhouse gases, and N<sub>2</sub>O contributes also to ozone depletion in the stratosphere.<sup>4,5</sup>

The present work is a continuation of a project, previously published in refs 2 and 6. Characterizations of NO and N<sub>2</sub>O have been carried out simultaneously but, for convenience, results of the present work which are related to NO are reported separately.<sup>7</sup>

The N<sub>2</sub>O emission has been found to depend on the bed temperature. A higher temperature leads to lower emis-

sions of N<sub>2</sub>O, which is the reverse of the bed temperature dependence of NO. In ref 2 it was discussed if the N<sub>2</sub>O formation from volatile nitrogen species (especially HCN) or the heterogeneous reactions on char surface play an active role for the N<sub>2</sub>O formation. No definite answer to this question could be given. In ref 6 it was reported that the char loading of the boiler influenced the fuel-nitrogen conversion to N<sub>2</sub>O. This could be seen by comparing N<sub>2</sub>O emission results from tests in which three kinds of fuel of different volatile contents were used. The temperature dependence of N<sub>2</sub>O was shown to include not only the bed temperature at the bottom, but the entire combustion chamber. Finally, the dependence of oxygen concentration of the N<sub>2</sub>O emission was evaluated.

It was shown by Leckner et al.<sup>8</sup> that the decomposition of N<sub>2</sub>O in the cyclone depends upon the temperature level. An increase of the cyclone temperature by fuel gas injection leads to a substantial reduction of the N<sub>2</sub>O produced in the combustion chamber.

The present work is focused on the formation of N<sub>2</sub>O in the combustion chamber. Results from measurements in a 12-MW commercial-type CFB boiler are presented. These measurements include transient response tests in which there were changes of the fly ash recirculation and fuel feed rates. Gas concentration profiles of O<sub>2</sub>, CO<sub>2</sub>, CO, NH<sub>3</sub>, HCN, NO, and C<sub>1</sub> to C<sub>3</sub> hydrocarbons are also measured. The aim of the work is to continue the discussion of the importance of formation of N<sub>2</sub>O from the nitrogen-containing volatiles (e.g., HCN) as compared with the formation related to char.

## Formation and Destruction of N<sub>2</sub>O

The formation and destruction of N<sub>2</sub>O under fluidized bed conditions are not well understood. For gas flames, where the chemical reactions are homogeneous, there are

(1) Leckner, B.; Åmand, L.-E. in *Ninth International Conference on Fluidized Bed Combustion*; Mustonen, J. P., Ed.; The American Society of Mechanical Engineers: New York, 1987; p 891.

(2) Åmand, L.-E.; Andersson, S. In *Tenth International Conference on Fluidized Bed Combustion*; Manaker, A. M., Ed.; The American Society of Mechanical Engineers: New York, 1989; p 49.

(3) Linak, W. P.; McSorley, J. A.; Hall, R. E.; Ryan, J. V.; Srivastava, R. K.; Wendt, J. O. L.; Mereb, J. B. *J. Geophys. Res.* 1990, 95, 7533.

(4) Ramanathan, V.; Cicerone, J. R.; Singh, H. H.; Kiel, J. T. *J. Geophys. Res.* 1988, 90, 5547.

(5) Crutzen, P. J.; Howard, C. J. *Pure Appl. Geophys.* 1978, 116, 497.

(6) Åmand, L.-E.; Leckner, B. *Combust. Flame* 1991, 84, 181.

(7) Åmand, L.-E.; Leckner, B. Oxidation of Volatile Nitrogen Compounds during Combustion in Circulating Fluidized Bed Boilers. *Energy Fuels*, preceding paper in this issue.

(8) Leckner, B.; Gustavsson, L. N<sub>2</sub>O reduction with Gas Injection in Circulating Fluidized Bed Boilers. *J. Inst. Energy*, in press.

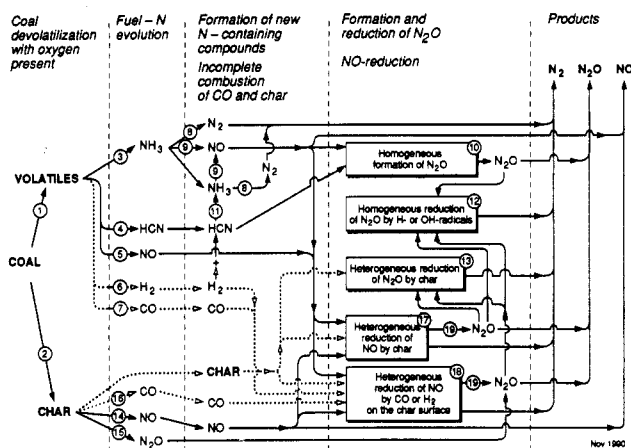


Figure 1. Pathways of fuel-nitrogen formation of  $N_2O$  in fluidized beds.

Table I. Important Formation and Reduction Steps for  $N_2O$  at Fluidized Bed Conditions<sup>a</sup>

reaction	catalyst	step in Figure 1	ref
formation of $N_2O$			
$HCN + O^* \rightarrow NCO^* + H^*$	homogeneous	10	10, 11
$NCO^* + NO \rightarrow N_2O + CO$	gas phase		
$2NO \rightarrow N_2O$	char	19	9, 12
$NO + \text{char-N} \rightarrow N_2O$	gas-solid reaction	19	9, 12
$\text{char-N} + (1/2)O_2 \rightarrow N_2O$	gas-solid reaction	15	12
reduction of $N_2O$			
$N_2O + H^* \rightarrow N_2 + OH^*$	homogeneous	12	10, 11
$N_2O + OH^* \rightarrow N_2 + HO_2^*$	gas phase		
$2N_2O + \text{char} \rightarrow N_2 + CO$	gas-solid reaction	13	12
other important reactions			
$2NH_3 + (3/2)O_2 \rightarrow N_2 + 3H_2O$	char	8	13
$NH_3 + (5/4)O_2 \rightarrow NO + (3/2)H_2O$	char	9	13
$HCN + 3H_2 \rightarrow NH_3 + CH_4$	homogeneous	11	14, 15
	gas phase		
$NO + \text{char} \rightarrow (1/2)N_2 + H_2O$	gas-solid reaction	17	13
$NO + CO \rightarrow (1/2)N_2 + CO_2$	char	18	13

<sup>a</sup> Reactions involving lime are excluded.

reaction schemes available<sup>9</sup> but the knowledge of the heterogeneous processes, which are more relevant for fluidized bed conditions, is poor. In a fluidized bed, there is not only coal present but also sand, ash, and lime, making interpretation even more difficult. As a simplification, limestone is not employed in the present experiments and sand is regarded to be rather inert, which leaves the char and ash as the only remaining surfaces of interest. Of these two surfaces, ash is regarded as less important than char.

In Figure 1 the important formation and reduction steps of  $N_2O$  under fluidized bed conditions are outlined. The scheme is based on the literature and detailed reactions and references can be found in Table I.

The scheme in Figure 1 shows the amount of fuel nitrogen which is released during combustion and found in the stack as  $N_2$ ,  $N_2O$ , and  $NO$ . On the left-hand side of Figure 1 the nitrogen content of the fuel is seen to be released either in the volatile fraction of the fuel, step 1, or in the char fraction, step 2. The volatile nitrogen is released in the form of intermediaries such as amines ( $NH_3$  in the scheme), step 3, or cyanides ( $HCN$  in the scheme), step 4, or oxidized directly to  $NO$ , step 5. The relation between the amounts of  $NH_3$  and  $HCN$  is important and depends on fuel type. Studies of bituminous coals<sup>16-18</sup> have shown that almost all coal nitrogen is contained in tightly bound heterocyclic rings such as pyridines and pyrroles, with small amounts of nitrogen contained in side chains. It is generally accepted that the primary nitrogen-containing product of pyrolysis of coal is  $HCN$ ,<sup>18-20</sup> apart from the nitrogen in the tar fraction, which remains in the same form as in the parent coal.<sup>17,18</sup> Measurements of the gas concentration profiles in staged pulverized coal flames<sup>21-23</sup> support the devolatilization studies and Bose et al.<sup>23</sup> stressed that, during oxidative pyrolysis conditions,  $NH_3$  is derived from  $HCN$  and  $HCN$  originates from the light gas fraction of the pyrolysis or from the tar nitrogen. The pyrolysis studies by Bauman and Möller<sup>14,15</sup> were closer to the situation existing in large fluidized beds than any of the work reported previously<sup>16,18,24,25</sup> Bauman and Möller<sup>14,15</sup> concluded that the primary nitrogen-containing species is  $HCN$  from the cleavage of heteroaromatic compounds and that  $NH_3$  can be formed by hydrogenation of  $HCN$ , step 11. This was also observed in oxidative pyrolysis studies, in the same experimental setup at a bed temperature of 600 °C. Similar formation of  $NH_3$  from  $HCN$  is modeled by Kilpinen and Hupa<sup>11</sup> for higher temperatures and shown experimentally under pulverized coal combustion conditions.<sup>18,23</sup> Furthermore, the calculations<sup>11</sup> indicate that there is a pathway from  $HCN$  to  $NO$  not shown in Figure 1.

The volatiles also contain  $H_2$  and  $CO$ , steps 6 and 7, which are important in the  $NO-N_2O$  chemistry as well. The  $NH_3$  formed is believed<sup>7</sup> to be oxidized to either  $NO$  or  $N_2$  on the char surfaces present, steps 8 and 9, and the homogeneous reduction of  $NO$  by  $NH_3$  is therefore considered less important and is excluded from the scheme. Laboratory studies of a similar oxidation of  $HCN$  on char surfaces are not found in the literature. Instead, the model calculations of  $N_2O$  formation at fluidized bed temperatures<sup>11</sup> show that  $HCN$  is the dominating nitrogen source for  $N_2O$ , step 10, whereas formation from  $NH_3$  is found to be significantly smaller. Experimental evidence of the formation route from  $HCN$  is given by Aho et al.<sup>26</sup> who

(16) Pohl, J. H.; Sarofim, A. F. *Proceedings of the Sixteenth Symposium (International) on Combustion*; The Combustion Institute: Pittsburgh 1977; p 491.

(17) Solomon, P. R.; Colket, M. B. *Fuel* 1978, 57, 749.

(18) Freihaut, J. D.; Seery, D. J. *Prepr. Pap.—Am. Chem. Soc., Div. Fuel Chem.* 1981, 12, 175.

(19) Axworthy, A. E.; Dyan, V. H.; Martin, G. M. *Fuel* 1978, 57, 29.

(20) Sugiyama, S.; Arai, N.; Hasatani, M.; Kawamura, S.; Kudou, I.; Matsuhiro, N. *Environ. Sci. Technol.* 1978, 12, 175.

(21) Chen, S. L.; Heap, M. P.; Pershing, D. W.; Martin, P. G. *Proceedings of the Nineteenth Symposium (International) on Combustion*; The Combustion Institute: Pittsburgh, 1982; p 1271.

(22) Glass, J. W.; Wendt, J. O. L. *Proceedings of the Nineteenth Symposium (International) on Combustion*; The Combustion Institute: Pittsburgh, 1982; p 1243.

(23) Bose, A. C.; Dannecker, K. M.; Wendt, J. O. L. *Energy Fuels* 1988, 2, 301.

(24) Blair, D. W.; Wendt, J. O. L.; Bartok, W. *Proceedings of the Sixteenth Symposium (International) on Combustion*; The Combustion Institute: Pittsburgh, 1977; p 475.

(25) Bauman, H.; Schuler, J.; Schiller, R. *Erdöl Erdgas Kohle* 1989, 105, 227.

(9) Kramlich, J. C.; Cole, J. A.; McCarthy, J. M.; Lanier, W. S.; McSorley, J. A. *Combust. Flame* 1989, 77, 375.

(10) Perry, R. A. *J. Chem. Phys.* 1985, 82, 5485.

(11) Kilpinen, P.; Hupa, M. Homogeneous  $N_2O$  Chemistry at Fluidized Bed Combustion Conditions—a Kinetic Modelling Study. *Combust. Flame*, in press.

(12) de Soete, G. G. *Proceedings of the Twenty-Third Symposium (International) on Combustion*; The Combustion Institute: Pittsburgh, 1990.

(13) Johnsson, J.-E. Kinetics of Heterogeneous  $NO_2$  Reactions at FBC Conditions. Report No 9003, Chemical Engineering Department, Technical University of Denmark, 1990.

(14) Möller, P. Verteilung von Stickstoffverbindungen bei der Pyrolyse von Steinkohlen unter Bedingungen der Wirbelschichtfeuerung. Dissertation, University of Essen, 1989.

(15) Bauman, H.; Möller, P. *Erdöl Kohle, Erdgas, Petrochem.* 1990, 44, 29.

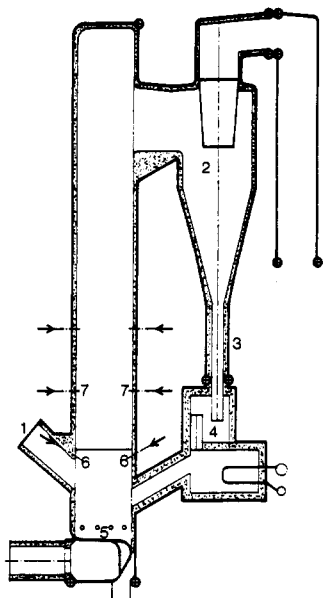


**Figure 2.** The 12-MW CFB boiler at Chalmers University of Technology: (1) fuel feed chute; (2) cyclone; (3) particle return leg; (4) particle seal; (5) bottom plate; (6) secondary air inlet at 2.2 m; (7) secondary air inlet at 3.8 m.

carried out tests in an entrained flow reactor with low particle loadings. The  $N_2O$  formed can be reduced either homogeneously with H and OH radicals, step 12, or heterogeneously on char surfaces, step 13.

As a simplification, the nitrogen in the char is assumed to produce only NO and  $N_2O$ , steps 14 and 15. The CO is produced from an incomplete combustion of the char, step 16, and the char itself is the main surface and reducing species for the reduction of NO to  $N_2$  in CFB boilers, steps 17 and 18. Then NO can be reduced to  $N_2O$  as well, step 19.

### Experimental Section

**The Boiler.** The tests were run in a 12-MW<sub>th</sub> boiler at Chalmers University of Technology, Figure 2. The boiler is built in the form of a commercial boiler with the combustion chamber made up of membrane tube walls which have a height of 13.5 m and a cross section of about 2.9 m<sup>2</sup>. Fuel is fed to the bottom of the combustion chamber through a fuel chute (1). The bed material entrained is separated from the gases in the hot cyclone (2) and passed back to the combustion chamber through the return leg (3) and the particle seal (4). Primary air is introduced through nozzles in the bottom plate (5) and secondary air can be injected through several registers located along the combustion chamber as indicated by the arrows in Figure 2. The lowest level (6) is located at 2.2 m and the second level (7) at 3.8 m. An additional cold cyclone, which is not seen in Figure 2, makes it possible to recycle fly ash back to the combustion chamber.

The boiler is equipped for research purposes with a data-acquisition system and on-line gas analyzers. The  $N_2O$  is measured with a continuous IR analyzer (Spectran 647 from Perkin Elmer). This analyzer is cross sensitive to methane in the gas;<sup>27</sup> therefore, gas-chromatograph analysis of  $N_2O$  was carried out as well. The  $N_2O$  analyzer has an extra large gas-sampling cell which gives a longer response time compared with the other gas analyzers. This makes it difficult to make on-line compensation in the  $N_2O$  signal for changes in oxygen concentration. Consequently the gas concentrations in the following figures are expressed as measured without conversion to a certain  $O_2$  concentration in the gas.

**The Tests.** A reference case was defined, for which the bottom bed temperature was kept at 850 °C, the primary air stoichiometry

was around 0.75, and the excess ratio was 1.2. The fluidizing velocity was 6 m/s. This reference case was used for all tests except for the case in which the fly ash recirculation was stopped, and a bed temperature of 830 °C, a primary-air stoichiometry of 1.0, and an excess-air ratio of 1.3 were used. The fuel was a bituminous coal of the following composition: ash, moisture and content of combustibles, 9.5%, 12.5%, and 78.0% respectively, analyzed as delivered; C, H, O, S, and N, 84%, 5%, 9%, 0.5%, and 1.9%, respectively, expressed on a moisture and ash-free basis (maf). The volatile content was 30% on the maf basis. The size of the coal was 0–30 mm with a mean size on a mass basis of 11 mm, and 13% of the fuel had a size less than 1 mm.

**The Gas-Sampling Probes.** The concentration profiles were measured inside the combustion chamber with gas-sampling probes. Gas was withdrawn through a cooled filter located at the top of the probe. The particle-free gas was then sent to on-line analysis for  $O_2$ , CO,  $CO_2$ , and NO. The HCN and  $NH_3$  profiles and the concentrations of  $C_1$  to  $C_3$  hydrocarbons were also measured. The  $NH_3$  and HCN concentrations were determined by trapping the gases in wash bottles containing a diluted acidic water solution for  $NH_3$  and a basic water solution for HCN. The analysis was then carried out by ion-selective electrodes for  $NH_3$  and argentometry (Liebig–Deniges method) for HCN. After drying, gas from the probes was also collected in Tedlar bags for further analyses of  $N_2O$  and hydrocarbons on a gas chromatograph equipped with an electron-capture detector (for  $N_2O$ ) and a flame-ionization detector (for hydrocarbons).

### Description of the Results

**Step Response Test with Stopped Fly Ash Recirculation.** Figure 3a–c shows the transient response of the concentrations of  $O_2$ ,  $CO_2$ , CO, NO, and  $N_2O$  together with the temperatures in the combustion chamber and the cyclone after stopping the fly ash recirculation. Before it was stopped, the fly ash recirculation had been kept at the same rate for more than 6 h and the char content of the fly ash had reached a steady state, which is seen in the figure, for a period of 9 min.

When the fly ash recirculation was stopped, the oxygen concentration increased from 6% to 8% (Figure 3a) and the  $CO_2$  concentration decreased correspondingly (Figure 3b) as a consequence of a loss of combustible matter. Part of this loss consists of fine particles which burned in the cyclone before the recirculation stop and the temperature of the gas leaving the cyclone dropped 50 °C after the stop (Figure 3a). Probably CO was also produced in the cyclone from an incomplete oxidation of the char in the fly ash, since the CO concentration dropped as well (Figure 3b).

In Figure 3c, the change of  $N_2O$  and NO can be followed. The increase of NO from 70 ppm (expressed at 6%  $O_2$ ) to 160 ppm was expected, judging from experience with fly ash recirculation in a similar CFB boiler,<sup>28</sup> but the corresponding decrease of the  $N_2O$  emission by 6% from 200 ppm (at 6%  $O_2$ ) down to 185 ppm came as a surprise. The decrease of  $N_2O$  occurred in spite of the increase of the oxygen concentration and the decrease of the temperature in the cyclone. Similar independent changes of these parameters lead to an increase of the  $N_2O$  emission. Tests on fly ash recirculation have also been carried out in a 1-MW<sub>th</sub> stationary (bubbling) fluidized bed boiler by Bramer and Valk.<sup>29</sup> They found the same influence on NO and  $N_2O$  as reported in the present work.

**Step Response Test with Batch Supply of Fuel.** Under stable operating conditions, a batch of fuel was dropped into the fuel chute together with the normal fuel

(28) Åmand, L.-E.; Leckner, B. *Proceedings of the Twenty-Third Symposium (International) on Combustion*; The Combustion Institute: Pittsburgh, 1990.

(29) Bramer, E. A.; Valk, M. *Eleventh International Conference on Fluidized Bed Combustion*; The American Society of Mechanical Engineers: New York, 1991; p 701.

(26) Aho, M.; Rantanen, J.; Linna, V. *Fuel* 1990, 69, 957.

(27) Hulgaard, T.; Dam-Johansen, K.; Karlsson, M.; Leckner, B. *Evaluation of an Infrared  $N_2O$  Analyzer*. Rep. No 8904, Dept. of Chem. Engineering, Technical University of Denmark, 1989.

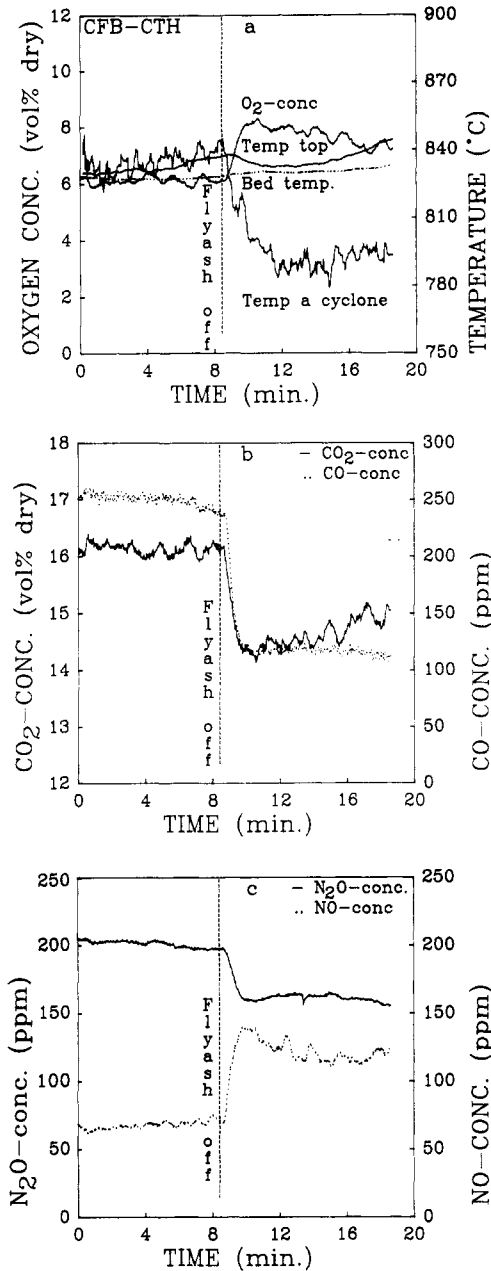


**Figure 3.** Step response test with stopped fly ash recirculation. Fly ash flow/fuel flow = 1.0. Operating conditions: bed temperature, 830 °C; excess air ratio, 1.3; primary air stoichiometry, 1.0.

feed. Not more than 30 s was required for the whole batch to be fed into the combustion chamber. The batch corresponds to an increase in the fuel feed rate of 2.3 times the normal rate. The normal fuel was used for batch fuel, but the size of the coal was varied. In the first test a coarse fraction was used, of a size between 15 and 40 mm, and in the second test the fine fraction, which was further crushed down to a mean size (mass based) of only 0.25 mm, was used. The results of both tests are shown in Figure 4, in the same way as the fly ash recirculation test. When the batch of fuel was dropped into the combustion chamber, the oxygen concentration decreased, Figure 4a, while the CO<sub>2</sub> concentration increased correspondingly, Figure 4b. The coarse fuel gave a much smaller O<sub>2</sub> peak, but the time needed for the O<sub>2</sub> to recover to its original level was much longer than the time needed for same amount of crushed fuel. The change of the temperatures can be followed in Figure 4a. The coarse fuel resulted in only a minor increase of the temperature in the top of the com-

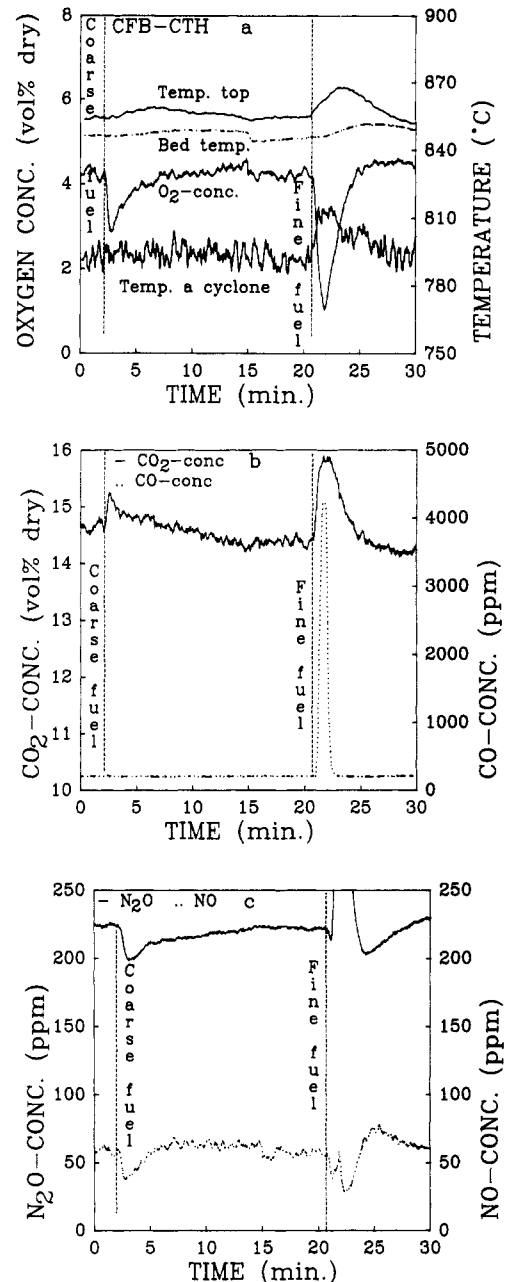


**Figure 4.** Step response test with batch supplies of bituminous coal. Batch size/fuel flow = 2.3. The N<sub>2</sub>O emission after the addition of the fine fuel is an artifact commented in the text. Operating conditions: reference case.

bustion chamber, in contrast to the fine fuel which caused an almost instantaneous increase of both the top temperature and the temperature of the gas leaving the cyclone. This is an effect of increased combustion in the cyclone, similar to that observed during the fly ash recirculation test. The bottom bed temperature also increased a little but, due to thermal inertia, this small increase was delayed a few minutes (Figure 4a).

The change of the CO concentration in the stack can be seen in Figure 4b. The coarse fuel, with its more prolonged devolatilization period, did not produce more CO than could be oxidized before the flue gas reached the stack. This is in contrast to the fine-sized fuel batch where a CO peak of 4000 ppm was produced.

The NO concentration decreased in both cases. A decrease of the N<sub>2</sub>O can be seen as well for the coarse-sized fuel batch, while a large N<sub>2</sub>O signal was recorded for the crushed fuel. However, this large peak does not represent

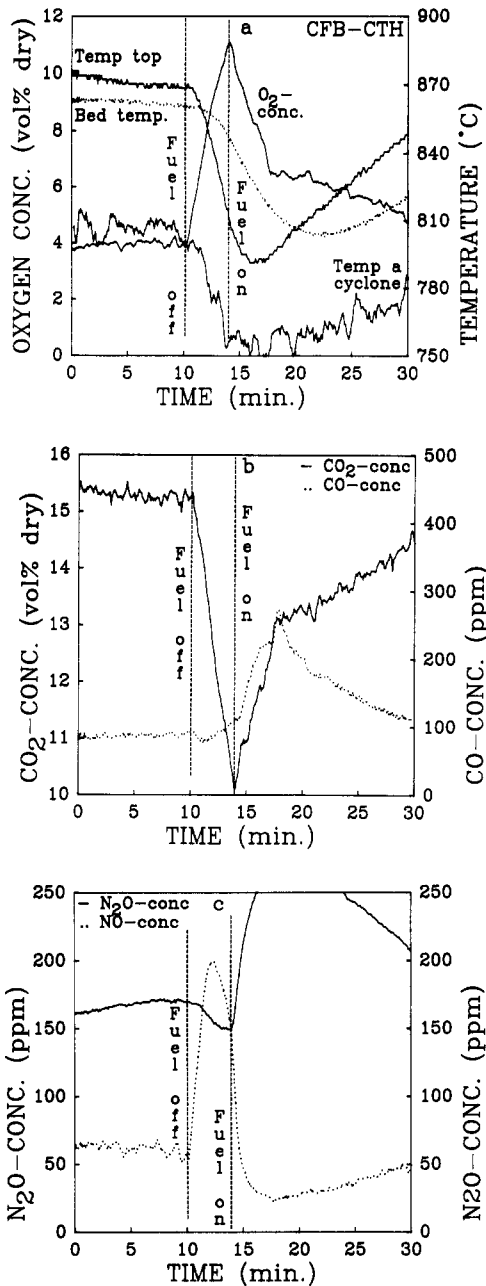


**Figure 5.** Step response test with stop and start on fuel feed. Operating conditions: reference case.

an increase in the  $N_2O$  concentration but is an influence on the IR analyzer from  $CH_4$  emitted by the sudden release of volatiles from the crushed coal. Both the  $CH_4$  emission and an actual decrease of the  $N_2O$  concentration were confirmed by gas-chromatograph measurements. The level of  $N_2O$  actually had decreased to 60 ppm, which is the correct value of  $N_2O$  at the time 22 min in Figure 4b.

**Step Response of the Stop and Start of the Fuel Feed.** The last series of step response tests are shown in Figure 5. The control system of the boiler was switched to manual mode, in order to prevent changes of the air and the flue-gas recirculation flows. The fuel was stopped for a period of four minutes. The heavy drop of the temperatures in the combustion chamber limits the time interval for the shut-off time of the fuel supply without a total turn down of the boiler. If the boiler stops, a restart would be needed and half of the step response test would be spoiled. The critical time was investigated in some preliminary tests. After 4 min without fuel supply, the fuel feed was started again at the same rate as during the

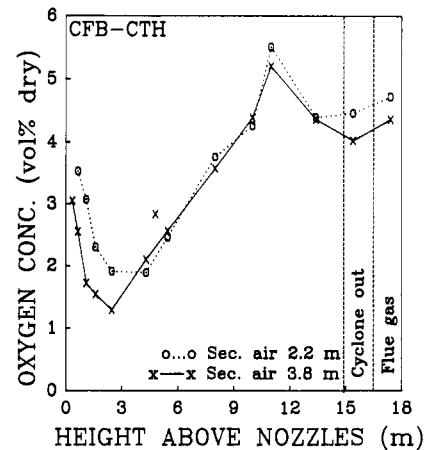


**Figure 6.** Oxygen concentration in the center of the combustion chamber with secondary air at 2.2 or 3.8 m. Operating conditions: reference case.

steady-state operation, and no extra fuel was supplied to speed up the recovery period. The control system was switched on after 15 min and stable operating conditions were attained after another 30 min. This period is not included in the figure in order to increase the resolution of the more interesting parts of the transient. As can be seen in Figure 5a, a stop of the fuel feed caused the oxygen concentration to increase from 4% to 11% and the  $CO_2$  to fall from 15.5% to 10% (Figure 5b). The CO concentration remained almost unchanged until the drop of the top temperatures became large. The CO increased even more when the fuel feed was started again and a release of large amounts of CO from the volatiles at low combustion temperatures occurred.

The NO concentration (corrected to 6%  $O_2$ ) increased from 60 to 200 ppm. The decrease of the NO concentration, after the peak (one minute before the fuel supply was started), was probably due to the falling combustion temperatures; however, the NO decrease was enhanced even more when the fuel supply was started again. For  $N_2O$  the opposite behavior was seen. The first decrease of  $N_2O$  was not more than can be explained as a dilution effect; however, when the fuel supply was restarted, an increase of the  $N_2O$  emission up to 280 ppm (at 6%  $O_2$ ) was recorded, which should be compared with the reference level of  $N_2O$  150 ppm (at 6%  $O_2$ ), before the start of the step-response test. The increase of  $N_2O$  observed in this case should be compared with the  $N_2O$  emission when batches of fuel were supplied and the emission decreased (Figure 4). A check for  $CH_4$  in the flue gas was carried out in this case as well, but none was found.

**Measurement of Gas Concentration Profiles in the Combustion Chamber.** Figure 6 shows the oxygen concentration profiles in the center of the combustion chamber when the height of the secondary air supply was changed. The profile looks different from oxygen-concentration profiles obtained in a laboratory-scale CFB combustor by Suzuki et al.<sup>30</sup> They measured falling oxygen-concentration profiles above the secondary air supply as well. The reason for this difference between the small laboratory unit with a diameter of only 0.1 m and the large 12-MW boiler can be found in the secondary air penetration. This is illustrated in Figure 7, which shows the horizontal profiles of oxygen at heights of 4.8 m (lower figure) and 8.0 m (upper figure), when the secondary air was supplied to the

(30) Suzuki, T.; Ishizuka, H.; Hyvarinen, K.; Morita, A.; Yano, K.; Mirose, R. *2nd SCEJ Symposium on Fluidized Beds*; Chemical Engineers of Japan: Tokyo, 1988; p 109.

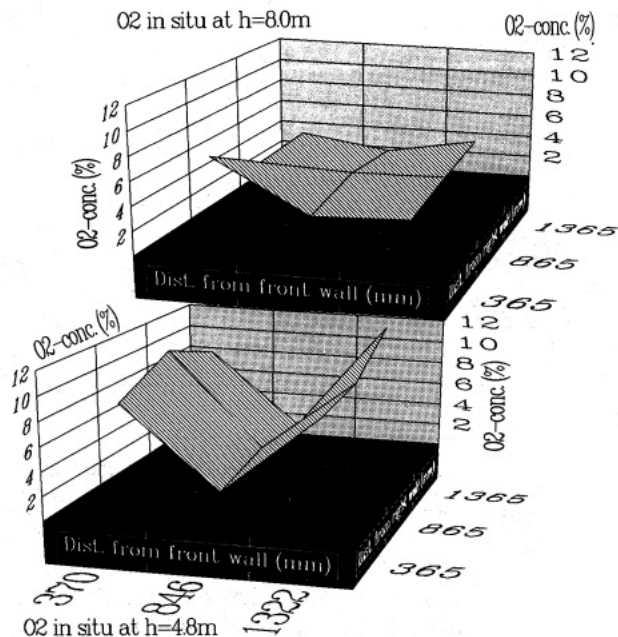


**Figure 7.** Horizontal profiles of oxygen at 4.8 and 8.0 m above the bottom of the combustion chamber. Secondary air is supplied at 3.8 m. Depth of figure shows the distance from the right wall. Operating conditions: reference case.

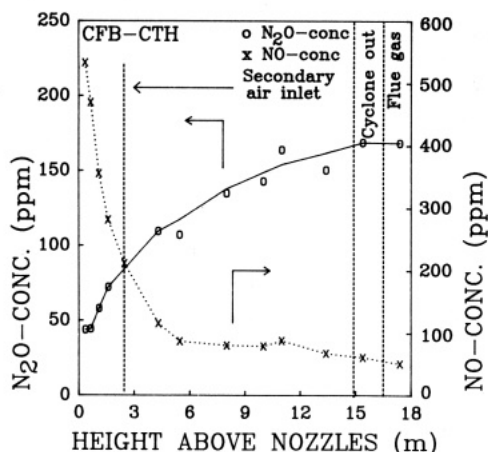


**Figure 8.** N<sub>2</sub>O and NO concentration profiles in the center of the combustion chamber with secondary air at 2.2 m. Operating conditions: reference case.

3.8-m level. The base plane of Figure 7 is the cross section of the combustion chamber. Secondary air is introduced from the front and rear walls of the combustion chamber. One meter above the secondary air nozzles, an increase of the oxygen concentrations could be registered at the six measurement points located parallel to the front and rear walls at a distance of 0.37 m from the walls. Along the center line located 0.85 m from the walls no change of oxygen was observed. Moving another 3.2 m upwards, a more even concentration profile could be seen as well as a higher average oxygen concentration along the center line. This means that more oxygen is transported to the middle of the combustion chamber from the oxygen-rich sides than the amount consumed by combustion. Measurement of horizontal profiles was carried out at the same time for CO<sub>2</sub>, CO, and NO as well, but not for the N<sub>2</sub>O because of interference from high CH<sub>4</sub> concentrations in the IR analyzer.

The CO<sub>2</sub> profiles are the inverse of the oxygen profile. Both the CO and NO were influenced by the large differences in oxygen concentration. At the center lines higher CO concentrations and lower NO concentrations

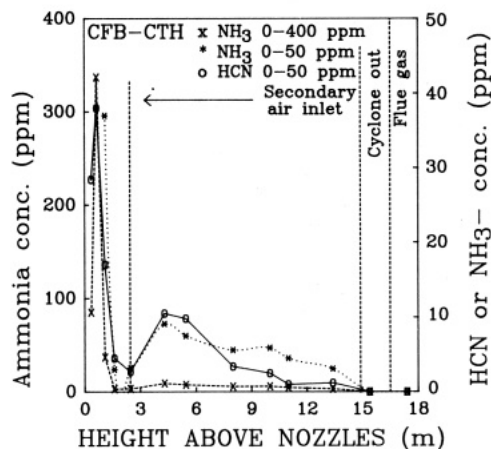


**Figure 9.** NH<sub>3</sub> and HCN concentration profiles in the center of the combustion chamber with secondary air at 2.2 m. NH<sub>3</sub> concentration is shown at 0–400 ppm range on left axis and 0–50 ppm range on right axis. Operating conditions: reference case.

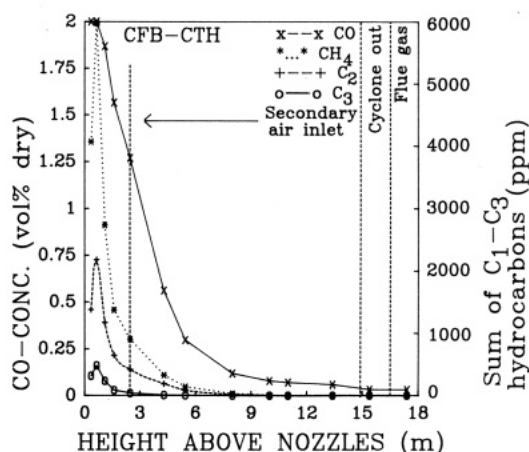


**Figure 10.** CO and C<sub>1</sub> to C<sub>3</sub> hydrocarbon concentrations in the center of the combustion chamber with secondary air at 2.2 m. Operating conditions: reference case.

were measured than at the oxygen-rich sides of the combustion chamber. The measurement in the middle of the combustion chamber (one point) is representative for the whole center line. This center line represents about 10% of the cross-section area of the combustion chamber. The remaining vertical profiles of NO, N<sub>2</sub>O, HCN, NH<sub>3</sub>, CO, and C<sub>1</sub> to C<sub>3</sub> hydrocarbons were recorded only in the middle of the combustion chamber, but these profiles are most likely representative for the center line as well.

Figure 8 shows the vertical profiles of N<sub>2</sub>O and NO. High concentrations of NO were found near the bottom but the NO decreased higher up in the combustion chamber as an effect of reducing reactions and dilution by secondary air, which is gradually mixed with the primary air. On the other hand, only 50 ppm of N<sub>2</sub>O was measured at the bottom and a slow increase of the concentration was seen along the upper part of the combustion chamber in spite of the dilution effect of secondary air. Similar profiles of NO and N<sub>2</sub>O from the combustion chamber of an 8-MW<sub>th</sub> CFB boiler have been reported<sup>2</sup> and have also been confirmed for a small laboratory unit with a diameter of only 0.1 m.<sup>31</sup>

In Figure 9 the concentrations of NH<sub>3</sub> and HCN can be followed. A rapid formation of these species occurred near

(31) Moritomi, H.; Suzuki, Y.; Kido, N.; Ogisu, Y. In *Circulating Fluidizing Bed Technology III*; Basu, P., Horio, M., Hasatani, M., Eds.; Pergamon Press: Oxford, U.K., 1991.

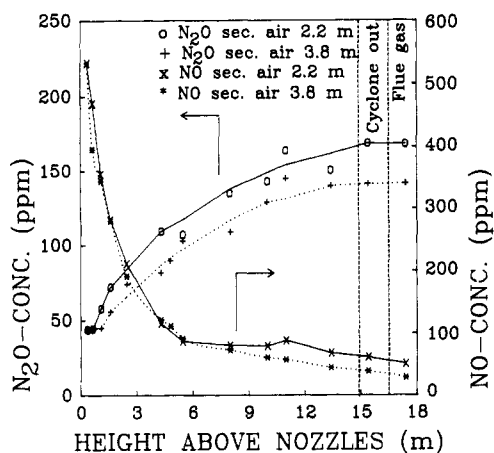


Figure 11. Comparison of the vertical profiles of N<sub>2</sub>O and NO at different heights of secondary air supply. Operating conditions: reference case.

the bottom, followed by an almost immediate decrease down to only about 5 ppm. The NH<sub>3</sub> dominated over the HCN and the ratio of NH<sub>3</sub>/HCN at the maximum concentrations (at  $h = 0.65$  m) was 8.5. When the secondary air starts to reach the center line, a second small maximum in the NH<sub>3</sub> and HCN concentrations was observed. Here the ratio of NH<sub>3</sub>/HCN is 1.0. The hydrocarbon concentrations also showed a large maximum at 0.65 m above the bottom of the combustion chamber (Figure 10). The ratios of the three classes of hydrocarbons at the maximum were CH<sub>4</sub>/C<sub>2</sub> = 2.7 and CH<sub>4</sub>/C<sub>3</sub> = 12. The hydrocarbons were oxidized almost completely before the secondary air reached the center line. The levels of CO were between 2% and 500 ppm in the combustion chamber. A maximum of CO could not be registered, since the CO instrument reached its upper limit. The decrease of CO is much slower than that of the hydrocarbons. There are three reasons for this. First, CO is produced as an intermediate of hydrocarbon oxidation. Second, the CO oxidation is a much slower reaction than the corresponding oxidation steps of hydrocarbons. Third, CO is also produced from an incomplete combustion of char and this char combustion takes place higher up in the combustion chamber, as well as at the bottom. Finally, a comparison of the N<sub>2</sub>O and NO profiles when the secondary air was supplied to different heights can be followed (Figure 11). Moving the secondary air to a higher level caused the N<sub>2</sub>O to increase more slowly to a lower level of 128 ppm (corrected to 6%), which is lower than the case shown in Figure 8 where an N<sub>2</sub>O concentration of 155 ppm (at 6%) was recorded. The NO profiles were very similar up to the 6-m level from which the NO decreases faster for the case of secondary air at 3.8 m. The exit concentration of NO dropped 45%, from 47 ppm (at 6% O<sub>2</sub>) down to 26 ppm (at 6% O<sub>2</sub>).

### Interpretation of the Results

**General.** It is assumed that there are two principal formation routes for N<sub>2</sub>O in CFB boilers, formation involving char and formation from HCN. The formation involving char can be either a direct consequence of the combustion of char and the conversion of fuel nitrogen according to step 15 (Figure 1) or a result of NO reduction with the char surface serving as a catalyst, step 19.

The results presented in Figures 3–11 are analyzed for the purpose of better understanding the two formation routes of N<sub>2</sub>O and summarized in Table II. It is evident, however, that the observations are affected by the reduction of N<sub>2</sub>O as well. One of the most extreme examples is given by Leckner and Gustavsson<sup>8</sup> where the homogeneous reduction with radicals (step 12, Figure 1) was

Table II. Support for N<sub>2</sub>O Formation Mechanisms

sort of test	figure (ref)	N <sub>2</sub> O formation		
		step 10, Figure 1	step 19, Figure 1	step 15, Figure 1
stop of fly ash recirculation	3, (29)		x	x
batch supply of fuel	4	x		
stop of fuel supply	5	x	x	
start of fuel supply	5	x	x	
NO, N <sub>2</sub> O profiles in combustion chamber	8, (2), (31)	x	x	x
NH <sub>3</sub> , HCN profiles in combustion chamber	9		x	x
secondary air, different levels	11	x		
NO doping of fluidizing air	(2), (32)		x	
tests with three different fuels	13	x	x	x

utilized to reduce N<sub>2</sub>O by firing of fuel gas in the cyclone apart from the processes in the combustion chamber.

**N<sub>2</sub>O Formation from Char.** Several test results indicate that the char content in the combustion chamber influences the formation of N<sub>2</sub>O.

Evidence of the influence of char is given by the step-response test with fly ash recirculation (Figure 3). Here, an N<sub>2</sub>O reduction was recorded as a consequence of the decrease of the amount of char when the recirculation was stopped, in spite of a simultaneous decrease in cyclone temperature. A change in cyclone temperature has been shown by independent tests<sup>8</sup> to have an effect on N<sub>2</sub>O which is opposite from that shown in Figure 3, and this further supports the influence of char, since fuel volatiles are insignificant in the cyclone under the present test conditions.

The vertical concentration profiles, Figures 8–11, indicate that the concentration of HCN is small in the upper part of the combustion chamber, which supports the assumption that the increase of N<sub>2</sub>O with height is a result either of char combustion or of reduction of NO on char surfaces. The continuous decrease of NO as the N<sub>2</sub>O increases supports the idea that the latter source of N<sub>2</sub>O plays a role through step 19 (Figure 1). Figure 11 shows that the NO concentration was decreased by 400 ppm between 1 and 5 m above the bottom of the combustion chamber, while the N<sub>2</sub>O increased by 50 ppm (in the case of secondary air at 3.8 m). Assuming the mechanism of Kramlich,<sup>9</sup> in which NO reacts with char nitrogen to form N<sub>2</sub>O (see Table I), one molecule of NO reduced is needed in order to produce one molecule of N<sub>2</sub>O and 12% of the NO reduced would produce the 50 ppm N<sub>2</sub>O. If instead NO molecules are adsorbed on the char surface, two moles are needed and 24% of the NO reduced would be spent to produce N<sub>2</sub>O. It can be seen that these conversions are possible at least from a mass-balance point of view.

The tests with stop and start of the fuel feed (Figure 5) can be interpreted as an effect of char as well as of volatiles. If formation of N<sub>2</sub>O as a consequence of NO reduction on char surfaces is relevant, the following interpretation could partly support the observations: When the fuel was stopped, the NO increased in spite of a decreasing release rate of fuel nitrogen and falling temperatures (Figure 5c). This is explained as an effect of the fast decrease of the CO levels noticed by measurements in the combustion chamber (but not seen in the exit CO concentration plotted in Figure 5b) and, thus, a lower reduction rate of NO on char surfaces. The corresponding decrease of N<sub>2</sub>O is partly hidden by the influence of the drop in the temperature but, on the other hand, when the fuel feed was started again, the NO reduction on char surfaces reappeared and a heavy

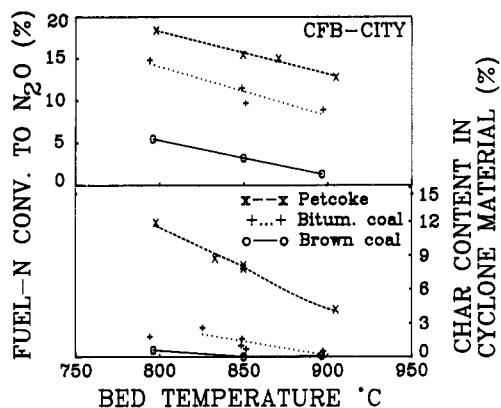


**Figure 12.** Fuel-nitrogen conversion to  $N_2O$  and char content in the material returning from the hot cyclone as a function of bed temperature for three different fuels. Operating conditions: reference case. Rewritten from data of Amand et al.<sup>6</sup>

increase of the  $N_2O$  emission was observed, which was certainly also caused to some extent by the volatiles.

A few results observed in previous tests support the discussion of the influence of char.

In the parameter study<sup>6</sup> three fuels with different volatile contents were used. In order to compare the fuels with each other, the results are rewritten in Figure 12 in the form of fuel-nitrogen conversion to  $N_2O$ . The char content of bed material taken from the return leg of the hot cyclone is plotted in Figure 12 as well. It is evident that the conversion of fuel nitrogen to  $N_2O$  is related to the char content. However, also in this example other factors may also influence the  $N_2O$  trends observed.

The only available test in which the  $N_2O$  formation from NO reduction is isolated from other influencing factors is taken from ref 2, where the fluidizing air was doped with 2200 ppm of NO. In the case in which bituminous coal was used as fuel, 85% of the NO added was reduced to  $N_2$ , but 5% was found as  $N_2O$ . Similar NO doping tests have been carried out in a laboratory fluidized bed<sup>32</sup> and similar results were obtained. The conversion of 5% is not the primary formation of  $N_2O$ , since reduction of  $N_2O$  (steps 12 and 13, Figure 1) is expected to occur also.

**$N_2O$  Formation from HCN.** Homogeneous formation of  $N_2O$ , step 10, Figure 1, is a possible route. In the calculations by Kilpinen and Hupa,<sup>11</sup> 500 ppm of HCN was needed to form about 100 ppm  $N_2O$  at 800 °C. The maximum values of HCN measured in the present tests never exceeded 40 ppm (Figure 9) and the HCN levels rapidly decreased with height in the combustion chamber to 10 ppm, without a corresponding increase of the concentrations of  $N_2O$ . It appears then that the relationship between the quantities of HCN needed, according to calculations, for an essential contribution to  $N_2O$  formation, and the measured values of HCN require further discussion.

The first question to be answered is whether the relation between the measured concentrations of  $NH_3$  and HCN is reasonable. It was mentioned above that  $NH_3$  could be produced from HCN by hydrogenation. This may be an explanation for the high concentrations of  $NH_3$  measured at a height of 0.65 m in the 12-MW boiler. Actually, the  $NH_3$  produced from the side chains of the coal structure (amino groups) may not be sufficient to reach the 350 ppm

level measured. If data from Bauman and Möller<sup>15</sup> concerning the  $NH_3$  yield in the light gas fraction from pyrolysis of bituminous coal are applied, a maximum concentration of 200 ppm  $NH_3$  in the primary zone of the 12-MW CFB boiler would be obtained. Fast hydrogenation of HCN may be an explanation of the high  $NH_3$  levels measured; however, the  $N_2O$  formation route from HCN still does not explain the levels of  $N_2O$  measured in the boiler. Further measurements of HCN are needed in the 12-MW boiler in order to cover a larger part of the bottom zone area, since higher HCN concentrations can be expected closer to the fuel-feed point. Furthermore, a conversion of HCN to  $NH_3$ , either on the filter of the probe or in the gas sampling probe itself, cannot be excluded in spite of the cooled probe used.

Although the HCN measured seems to be insufficient to explain a large part of the  $N_2O$  emission, besides the NO reduction on char other factors may play a role, such as heterogeneous reduction to  $N_2$  during reducing conditions. Examples of this are shown in Figure 11 where the increase in the height of the primary air zone by moving the secondary air to a higher level resulted in a decrease in both the NO and the  $N_2O$  emission. Similarly, in the batch supply tests shown in Figure 4, the NO and the  $N_2O$  emissions decreased simultaneously.

The trends in Figure 5, especially the ones observed when the fuel feed was restarted at an oxygen level of 11%, need further comment. In addition to what was said about the influence of char, the large values of  $N_2O$  could also be a result of a contribution from HCN according to step 10 (Figure 1) if the hydrogen released from the volatiles is predominantly oxidized to water in the oxygen-rich atmosphere, instead of converting HCN into  $NH_3$ .

The results in Figure 12, showing the  $N_2O$  emissions from fuels with different volatile contents, could possibly have been influenced also by the volatiles. The comments which follow are unfortunately simply speculations. The high conversion of fuel nitrogen to  $N_2O$  in the case of petroleum coke could be a partial result of a low release of  $H_2$ , which means that relatively more HCN would be available for  $N_2O$  formation. In the case of brown coal which is characterized by a low  $N_2O$  emission in spite of a high volatile content, a larger proportion of the volatiles might have been released as  $NH_3$ , since more fuel nitrogen is contained in the side chains of the brown coal compared with fuels of higher rank.

## Discussion and Conclusions

The tests were carried out in a bed of sand ash without addition of limestone.

**Formation-Destruction of  $N_2O$ .** Among the homogeneous reduction mechanisms, the reduction of  $N_2O$  by radicals is deemed to be the most important one.<sup>8</sup> The heterogeneous reduction of  $N_2O$  on char surfaces (step 13) was found by de Soete<sup>12</sup> to be higher than that of NO in his fixed bed reactor, in the absence of CO. This may shift to a higher NO reduction in the combustion chamber of a CFB boiler, with CO concentrations between 20 000 and 500 ppm. However, if formation and reduction are compared, it is evident that formation is dominant in the combustion chamber, since the  $N_2O$  concentration increases with height according to Figure 8.

**Conversion of HCN.** For the formation of  $N_2O$ , HCN is important at least in a homogeneous reaction situation. However, laboratory scale studies show that hydrogenation of primary produced HCN to  $NH_3$  may occur, which would withdraw HCN from the  $N_2O$  formation route.

**HCN versus Char.** There are no verifications of the importance of HCN for  $N_2O$  production in the heteroge-

(32) Ivarsson, E.-L.  $NO_x$  and  $N_2O$  Emissions from a Pressurized Bench-Scale Fluidized Bed Reactor. Thesis for the Degree of Licentiate of Engineering, Dept. of Energy Conversion, Chalmers University of Technology, 1990.

neous surrounding of a fluidized bed. Also, the low concentrations of HCN measured indicate that its importance may be limited. Measurement errors and strong concentration variations in the horizontal plane have to be further checked, however.

The char appears to be more important than HCN for the successive formation of N<sub>2</sub>O seen in Figure 11. It was mentioned above that a conversion of 10-30% of the NO converted by char would be sufficient to explain the N<sub>2</sub>O formation. This should be considered in relation to a possible contribution from char combustion (step 15). de Soete<sup>12</sup> has found that up to 5% of the char nitrogen was converted to N<sub>2</sub>O in his experiments. This value corresponds to 50 ppm of N<sub>2</sub>O assuming a complete combustion of the char. The figure of 5% is too small to explain the increase of the N<sub>2</sub>O concentration with height as an effect of char combustion only.

The general conclusion of this discussion is that there are several factors which indicate that the principal contribution to the N<sub>2</sub>O emission originates from the reduction of NO on char surfaces. Contributions from char combustion and HCN appear to be only of minor importance. This conclusion has to be further verified, of course, since the basic knowledge of N<sub>2</sub>O formation and reduction still has to be improved.

**Acknowledgment.** This work was financially supported by the Swedish National Energy Administration. The contribution to the experimental work by the operating staff of the boiler together with personnel from the Department of Energy Conversion is gratefully acknowledged.

**Registry No.** N<sub>2</sub>O, 10024-97-2; CO<sub>2</sub>, 124-38-9; CO, 630-08-0; NO, 10102-43-9; HCN, 74-90-8; NH<sub>2</sub>, 7664-41-7.

---

## Aqueous High-Temperature Chemistry of Carbo- and Heterocycles. 16.<sup>1</sup> Model Sulfur Compounds: A Study of Hydrogen Sulfide Generation

Alan R. Katritzky,\* Ramiah Murugan, Marudai Balasubramanian, and John V. Greenhill

*Department of Chemistry, University of Florida, Gainesville, Florida 32611-2046*

Michael Siskin\* and Glen Brons

*Corporate Research Science Laboratory, Exxon Research and Engineering Company, Annandale, New Jersey 08801-0998*

*Received December 11, 1990. Revised Manuscript Received August 13, 1991*

---

The aquathermolysis reactivity of nine organic sulfur compounds was investigated to determine their potential to generate hydrogen sulfide during the cyclic steam stimulation process to recover Cold Lake bitumen. Dioctyl sulfide, 1-decanethiol, didecyl disulfide, 1-naphthalenethiol, 1,1'-dinaphthyl sulfide, 1,1'-dinaphthyl disulfide, 1-naphthyl 1-octyl sulfide, tetrahydrothiophene, and thiophene were selected as model compounds and subjected to neutral, basic, and acidic aquathermolysis conditions at 250 and 300 °C. Thiols, and thiols formed by cleavage of sulfides and disulfides, were found to be the source of H<sub>2</sub>S evolution. Aliphatic sulfides, in addition to their usual C-S bond cleavage, showed  $\alpha,\beta$  C-C bond cleavage. Nontronite clay was found to catalyze all cleavages at 300 °C and to catalyze aromatic sulfide isomerization. Tetrahydrothiophene and thiophene were inert under all the reaction conditions investigated. It is shown that there is a significant increase in H<sub>2</sub>S production as the temperature is raised from 250 to 300 °C for all substrates and conditions. To minimize the escape of H<sub>2</sub>S to the atmosphere, the steam stimulation processes should be run at as low a temperature as possible.

---

### Introduction

Organic sulfur levels in Cold Lake bitumen (CLB) are high (4-7 wt %). This sulfur is distributed largely as thiophenes (75%), sulfides (25%), and as thiols and disulfides (<<1%). Environmentally unacceptable levels of hydrogen sulfide are produced during the latter stages of a production cycle in the cyclic steam stimulation process (CSS) at Cold Lake. This has prompted us to carry out fundamental studies to determine the potential organic

sources of the H<sub>2</sub>S in order to learn how to control its evolution.

During the CSS process, superheated steam (80%) and an aqueous brine at pH ca. 10.5 (20%) are injected into the Clearwater formation at 315 °C for about 30-50 days to enhance the recovery of bitumen. The injection fluid heats the deposit which decreases the viscosity of the bitumen to facilitate recovery. This cycle is repeated several times with the levels of the H<sub>2</sub>S in the unscrubbed gas gradually increasing above 0.1 wt %, which is the limit set by the Alberta government.

To define the types of organic molecules that produce hydrogen sulfide under the CSS conditions employed at

---

(1) Katritzky, A. R.; Murugan, R.; Siskin, M. *Energy Fuels* 1990, 4, 577.